Journal of Catalysis **189,** 70–78 (2000)
Article ID jcat.1999.2685, available online at http://www.idealibrary.com on IDEAL®

Hydrodenitrogenation Activities of Methyl-Substituted Indoles

S. C. Kim and F. E. Massoth[1]

Department of Chemical and Fuels Engineering, University of Utah, Salt Lake City, Utah 84112

Received May 21, 1999; revised September 1, 1999; accepted September 13, 1999

The hydrodenitrogenation (HDN) reactivities of indole (IND) and several methyl-substituted indoles (MIN) were determined over a $NiMo/Al_2O_3$ catalyst and a $CoMo/Al_2O_3$ catalyst using a fixed-bed reactor at 340°C and 31 atm hydrogen pressure. Appreciable differences in reactivity were obtained, depending on the location of the methyl group. Compared to IND, overall conversions and HDN conversions were generally higher when methyl groups were on the aromatic ring, and substantially lower for methyl groups on the N ring. Two paths for initial conversion of IND (MIN) were deduced, viz., a CNH path (C–N bond cleavage) and a HYD (aromatic hydrogenation) path. The NiMo catalyst favored the HYD path over the CNH path, while the opposite occurred for the CoMo catalyst. Reasonable trends were obtained between initial CNH rates and the electrostatic potential on the N atom of the MINs, and between initial HYD rates and the ionization potential.

Key Words: **indole; methyl-substituted indoles; hydrodenitrogenation (HDN); NiMo catalyst; CoMo catalyst; computational chemistry.**

INTRODUCTION

Catalytic hydrotreating has become an important process for removal of sulfur and nitrogen from petroleum due to increasing environmental constraints. The heterocyclic compounds of sulfur and nitrogen also have potential to cause corrosion and poisoning of downstream catalysts; therefore, there is a need for hydrotreating. Heterocyclic compounds containing sulfur and nitrogen are relatively stable structures because of their aromatic character. Even though the hydrotreating process removes sulfur and nitrogen simultaneously, nitrogen compounds are more resistant than sulfur compounds and require more severe reaction conditions. Although the importance of hydrodenitrogenation is gaining importance, less quantitative information is available on the catalytic chemistry of hydrodenitrogenation than that of hydrodesulfurization (HDS).

It is well-known that the difficulty in achieving high HDS conversions with conventional feeds is due to certain "unreactive" sulfur compounds. These have been identified as alkyl-substituted dibenzothiophenes in which the alkyl group is located on a carbon atom adjacent to the sulfur atom (1). Problems associated with these effects in achieving high HDS conversions have been recently addressed by Whitehurst *et al.* (2).

A number of studies have been reported on the effect of methyl groups on the hydrodesulfurization of model compounds such as thiophene (3), benzothiophene (4, 5), and dibenzothiphene (5–8). In these studies, it was found that methyl groups on C atoms adjacent to the S atom resulted in lower activity. It is believed that this is due to steric hindrance to adsorption through the S atom by the methyl group.

Only limited studies have been reported on the effect of alkyl substituents on hydrodenitrogenation (HDN) reactivity of model N-heteroatom compounds. Cerny (9) reported that the effect of methyl groups upon hydrogenolysis of methyl-substituted pyridines followed in the series pyridine > 2-methylpyridine > 2,6-dimethylpyridine > 2,4,6-trimethylpyridine, indicative of steric hindrance. Liaw *et al.* (10) reported the order of reactivity as pyridine > 2-methylpyridine > 3-methylpyridine; the latter compound should not exhibit steric hindrance if adsorption is through the N atom. Also, Bhinde (11) reported that the HDN reactivities of 2,6-, 2,7-, and 2,8-dimethylquinoline are comparable to that of quinoline. It is evident that steric effects alone cannot explain the reactivity of six-membered heterocyclic compounds. The effect of alkyl substituents on five-membered nitrogen compounds, such as indole, have not been reported.

The HDN of heterocyclic nitrogen compounds generally involves the following reactions: (1) hydrogenation of nitrogen heterorings, (2) hydrogenation of aromatic rings, and (3) C–N bond cleavage (12). Several studies using indole as a model compound for the HDN reaction have invoked various reaction pathways involving a sequence of coupled hydrogenation and hydrogenolysis steps (13–16). Recently, Zhang and Ozkan (17) proposed a more complex network, as shown in Scheme 1. A rapid hydrogenation of indole (IND) to indoline (HIN) is followed by two different paths, viz., direct hydrogenation of the aromatic ring of indoline to form octahydroindoline (OHI), which proceeds rapidly to another intermediate ethylcyclohexylamine (OECHA), followed by C–N bond rupture to form the intermediate

[1] To whom correspondence should be addressed.

0021-9517/00 $35.00

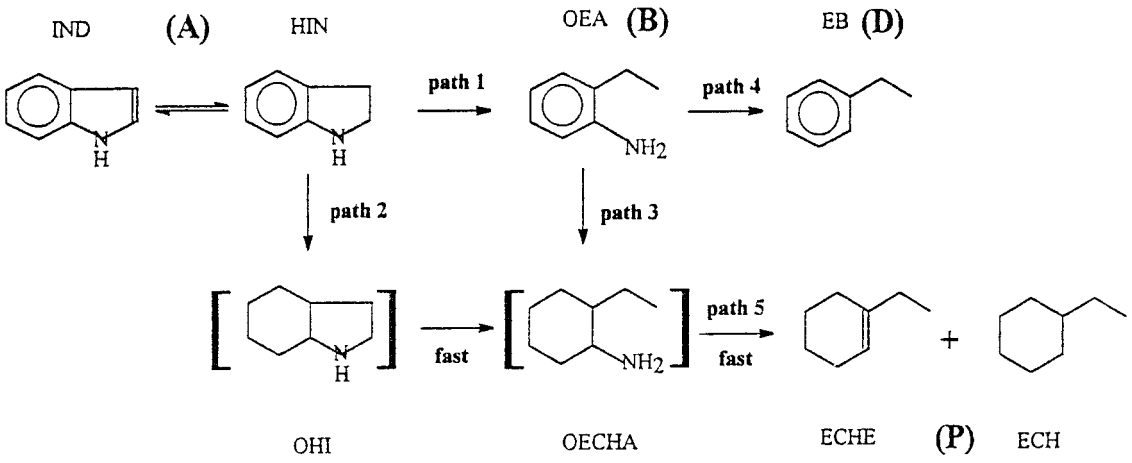

SCHEME 1. Suggested reaction pathways for the HDN of indole.

orthoethylaniline (OEA). The latter then reacts further by two paths, viz., direct denitrogenation leading to ethylbenzene (EB), or aromatic ring hydrogenation to ethylcyclohexylamine. The latter, forming from two paths, is very reactive and rapidly forms ethylcyclohexene (ECHE) and ethylcyclohexane (ECH). The difference between this scheme and previous ones is the proposal for reaction paths through the intermediates OHIN and OECHA, which were detected under certain reaction conditions (18).

The aim of the present study was to determine the effect of methyl substituents on the HDN of indole and attempt to explain the results. The numbering system for indole is shown below.

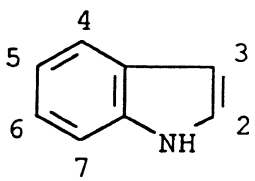

EXPERIMENTAL

The catalysts used were Topsøe TK-554, which consisted of 4.1% CoO and 20.5% MoO_3 supported on alumina (220 m^2/g), and Topsøe TK-555, which consisted of 3.8% NiO, and 24% MoO_3 supported on alumina containing 2% phosphorous (160 m^2/g). The 1.27-mm extrudates were crushed and sieved to 40- to 60-mesh particles. Reactions were carried out in a fixed-bed reactor at 340°C and 35 atm under vapor-phase conditions. Either a 0.25- or 0.1- g sample of catalyst, mixed with 5 cm^3 of glass beads, was presulfided with a 10% H_2S–90% H_2 mixture by volume under atmospheric pressure and 400°C for 2 h. The liquid feed consisted of 0.5 wt% of indole (IND) or methyl-substituted indole (MIN) and 1.0 wt% dimethyldisulfide, in *n*-heptane solvent. The hydrogen flow rate and liquid flow rate were varied proportionally so that a constant feed concentration was maintained throughout the run. After the catalyst was aged for 2 days under reaction conditions, catalyst activity remained essentially constant over 300 h. Liquid samples taken at various space times were analyzed by gas chromatography (30-m × 0.32-mm glass capillary column (Hewlett Packard, HP-1) containing dimethylpolysiloxane) and use of a flame ionization detector and temperature programming of 10°C/min. The identity of individual products was determined by comparison with pure reference samples and GC/MS analysis. Molar GC factors were determined using available samples of IND and its reaction products. The same relative factors were assumed to apply to the MINs.

The major compounds found in the samples from runs with indole were indole (IND), *o*-ethylaniline (OEA), two isomers of ethylcyclohexene (ECHE), ethylcyclohexane (ECH), and ethyl benzene (EB); analogous compounds containing a methyl group were found for runs with methyl indoles (MIN). Small amounts of the dihydroindoles (HIN or HMIN) were detected, and these were considered as the reactants together with IND or MIN. Total conversion (TOT) of IND or MIN was determined from the sum of the mole fractions of products, while HDN conversion was determined from the sum of the mole fractions of the non-N-containing products. Space time, τ, was defined as the weight of catalyst divided by the total gas flow (hydrogen plus vaporized liquid feed).

Modeling of the various indoles by computational chemistry was carried out on a PC platform, while ab initio calculations were done on an IBM-SP parallel supercomputer. The ground-state electronic properties of indole and the methyl-substituted indoles and their partially hydrogenated analogs were calculated using both Mopac (Chem-3D) and Gaussian 98. At first, the semi-empirical PM3 method was employed for initial geometry optimization. Subsequently, the geometry optimization was repeated with

Gaussian 98, using a Hartree-Fock SCF/6-31G(d) basis set. Further details are provided elsewhere (19).

RESULTS

A. *Reactivities of MINs*

Reactions of IND and various MINs were carried out with the NiMo catalyst at three space times using 0.25-g catalyst. Product distribution data are given in Table 1, and total (TOT) and HDN conversions of the various MINs are plotted in Fig. 1 for one space time. It is evident that the location of the methyl group has a significant effect on reactivity. The order of reactivities is as follows:

TOT conversion: 6-MIN > 5-MIN ~ 7-MIN ~ IND > 2-MIN ~ 2,5-MIN > 3-MIN,

HDN conversion: 6-MIN > IND ~ 5-MIN ~ 7-MIN ~ 2-MIN > 2,5-MIN > 3-MIN.

Thus, methyl groups on the aromatic ring slightly increase, while those on the N ring decrease in TOT conversion compared to IND. On the other hand, only the 6-MIN promotes HDN activity, while the 5- and 7-MIN have no effect; again methyls on the N ring decrease HDN. In the case of 2,5-MIN, evidently the effect of the 2-position overrides that of the 5-position. It is also evident from Fig. 1 that, for the HDN of indole, steric hindrance due to methyl groups adjacent to the N atom is not important in contrast to the relatively large effects found in the HDS of sulfur compounds.

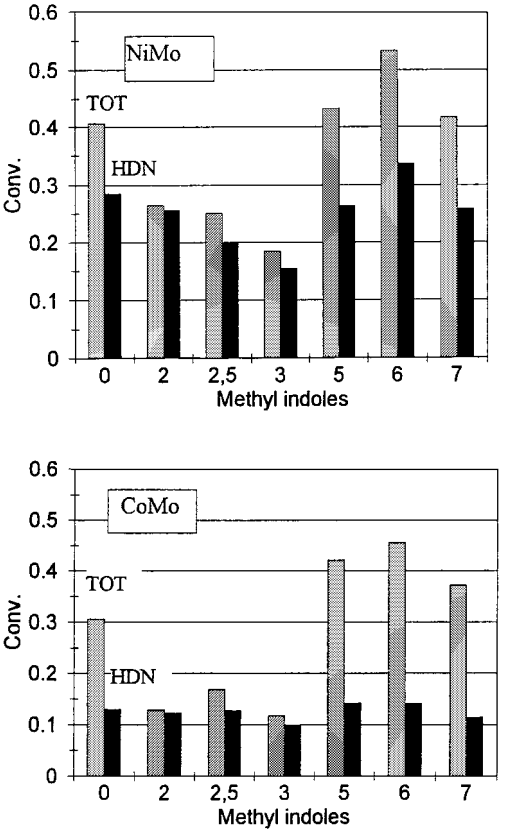

FIG. 1. Total (TOT) and HDN conversions of indole and methyl-substituted indoles. Numbers refer to the carbon atom on which the methyl group is attached.

TABLE 1

Product Distributions and Conversions of MINs for an NiMo Catalyst (340°C and 0.25 g of Catalyst)

							Conv.	
τ^a	Cpd.	IND + HIN	OEA	ECH	EB	ECHE	TOT	HDN
0.74	IND	0.593	0.122	0.129	0.015	0.141	0.407	0.285
	2-MIN	0.735	0.009	0.147	0.007	0.102	0.265	0.256
	2,5-MIN	0.749	0.050	0.072	0.021	0.108	0.251	0.201
	3-MIN	0.815	0.031	0.072	0.026	0.056	0.185	0.154
	5-MIN	0.568	0.169	0.056	0.016	0.192	0.432	0.264
	6-MIN	0.467	0.197	0.076	0.024	0.237	0.533	0.337
	7-MIN	0.582	0.160	0.075	0.018	0.165	0.418	0.258
1.11	IND	0.411	0.158	0.248	0.025	0.158	0.589	0.431
	2-MIN	0.538	0.010	0.321	0.015	0.116	0.462	0.452
	2,5-MIN	0.549	0.069	0.160	0.044	0.177	0.451	0.381
	3-MIN	0.694	0.034	0.163	0.038	0.07	0.306	0.271
	5-MIN	0.328	0.207	0.14	0.035	0.29	0.672	0.465
	6-MIN	0.267	0.233	0.156	0.043	0.302	0.733	0.501
	7-MIN	0.346	0.213	0.142	0.041	0.259	0.654	0.442
1.48	IND	0.276	0.17	0.371	0.034	0.149	0.724	0.554
	2-MIN	0.375	0.008	0.515	0.024	0.077	0.625	0.616
	2,5-MIN	0.420	0.078	0.239	0.046	0.216	0.580	0.501
	3-MIN	0.615	0.034	0.230	0.044	0.078	0.385	0.352
	5-MIN	0.172	0.189	0.233	0.053	0.353	0.828	0.639
	6-MIN	0.144	0.233	0.229	0.061	0.334	0.856	0.624
	7-MIN	0.255	0.227	0.183	0.049	0.286	0.745	0.518

[a] τ in (kg min)/m^3.

Changes in distribution of products for the various MINs can give further insight into the reason for the differences between TOT and HDN conversions. Figure 2 displays product distributions in terms of hydrogenated hydrocarbon products, aromatic hydrocarbons, and intermediate anilines. It is evident that the relatively low HDN responses for the 5-, 6-, and 7- MINs, as compared to their TOT conversions, is reflected in their greater yield of the intermediate aniline compound. That is, the aniline compound is formed faster than it reacts. For methyls on the N ring, there is relatively less anilines, and consequently their HDN conversions are not greatly different from their TOT conversions. Since the aromatic yields are small compared to the yield of the hydrogenated products, the latter predominates the HDN activity.

Reactions of IND and various MINs were carried out with the CoMo catalyst at several space times using 0.1 g of catalyst. Product distribution data are listed in Table 2, and total and HDN conversions of the various MINs are plotted in Fig. 1 for one space time. The order of reactivities is as

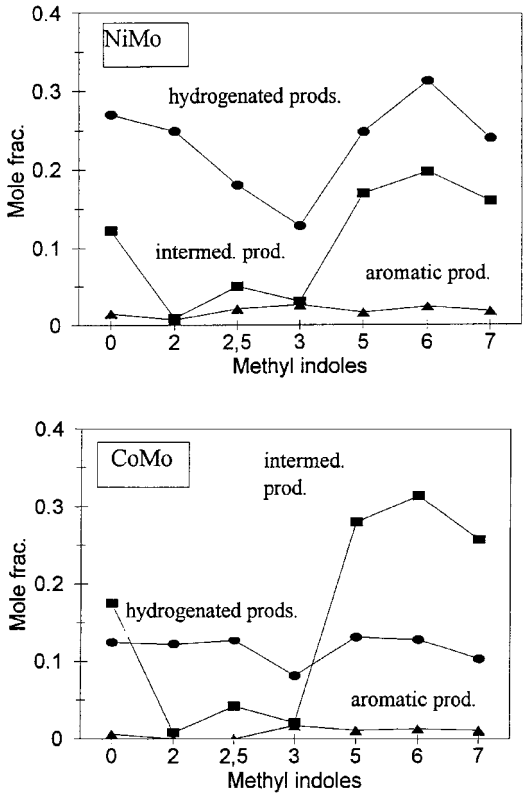

FIG. 2. Mole fractions of the reaction products vs the methyl position in the indoles. Hydrogenated products, ECHE + ECH; intermediate product, OEA; aromatic product, EB; also methyl analogs of these.

follows:

TOT conversion: 6-MIN > 5-MIN > 7-MIN > IND > 2,5-MIN > 2-MIN ~ 3-MIN,

HDN conversion: 6-MIN ~ 5-MIN > IND ~ 7-MIN ~ 2-MIN ~ 2,5-MIN > 3-MIN.

Again, methyl groups on the aromatic ring enhance, while those on the N ring repress TOT conversion compared to IND. In no case is HDN increased, although 5- and 6-MIN are about the same as IND. Large differences are observed between TOT conversion and HDN for methyl groups on the aromatic ring, while only small differences are observed on the N ring. Again, the major reason for the former lies in the relatively high OEA yields, as seen in the product distribution plot of Fig. 2.

Table 3 presents data on the reactivity of HIN vs IND under the same conditions. It is seen that there is no appreciable difference in reactivity whether starting with IND or with HIN. This indicates that the reaction between IND and HIN is in equilibrium and the conversion of IND to HIN is not a limiting step in the HDN of IND under our reaction conditions. Also given in Table 3 are data for 2-MIN vs 2-HMIN. Again, no difference in conversions is observed,

TABLE 2

Product Distributions and Conversions of MINs for a CoMo Catalyst (340°C and 0.1 g of Catalyst)

							Conv.	
τ^a	Cpd.	IND + HIN	OEA	ECH	EB	ECHE	TOT	HDN
0.277	IND	0.875	0.077	0.019	0.001	0.029	0.125	0.049
	2-MIN	0.961	0.005	0.021	0.000	0.014	0.039	0.035
	5-MIN	0.816	0.133	0.010	0.002	0.040	0.184	0.052
	7-MIN	0.837	0.128	0.008	0.003	0.023	0.163	0.034
0.341	IND	0.828	0.099	0.029	0.005	0.039	0.172	0.073
	2-MIN	0.951	0.008	0.026	0.000	0.015	0.049	0.041
	2,5-MIN	0.944	0.023	0.020	0.000	0.013	0.056	0.033
	3-MIN	0.964	0.011	0.011	0.006	0.007	0.036	0.024
	5-MIN	0.766	0.169	0.015	0.004	0.046	0.234	0.065
	6-MIN	0.754	0.193	0.014	0.004	0.036	0.246	0.054
	7-MIN	0.801	0.151	0.013	0.004	0.031	0.199	0.048
0.444	IND	0.780	0.125	0.046	0.003	0.046	0.220	0.095
	2-MIN	0.915	0.008	0.046	0.001	0.030	0.085	0.077
	2,5-MIN	0.891	0.036	0.042	0.001	0.030	0.109	0.073
	3-MIN	0.925	0.03	0.025	0.005	0.015	0.075	0.045
	5-MIN	0.694	0.213	0.024	0.007	0.061	0.306	0.092
	6-MIN	0.661	0.248	0.025	0.007	0.059	0.339	0.091
	7-MIN	0.735	0.188	0.019	0.006	0.053	0.265	0.078
0.634	IND	0.694	0.175	0.075	0.006	0.049	0.306	0.130
	2-MIN	0.871	0.008	0.083	0.000	0.039	0.129	0.122
	2,5-MIN	0.831	0.042	0.061	0.000	0.066	0.169	0.127
	3-MIN	0.883	0.021	0.065	0.017	0.016	0.117	0.098
	5-MIN	0.579	0.280	0.050	0.011	0.081	0.421	0.142
	6-MIN	0.545	0.314	0.044	0.013	0.084	0.455	0.141
	7-MIN	0.628	0.257	0.034	0.011	0.069	0.372	0.114
0.887	2,5-MIN	0.682	0.050	0.148	0.006	0.115	0.318	0.269
	3-MIN	0.840	0.021	0.106	0.017	0.017	0.160	0.140
	6-MIN	0.477	0.352	0.060	0.015	0.095	0.523	0.170

[a] τ in (kg min)/m^3.

indicating that the hydrogenation of 2-MIN to 2-HMIN is also not rate-limiting.

B. Initial Rates

Referring to Scheme 1, Scheme 2 was developed for the purposes of analysis of initial rates. As the intermediates, OHI and OECHA, were not detected under our reaction conditions, they are assumed to react fast.

Reaction product data, obtained for each MIN at three space times and one feed composition, are insufficient to

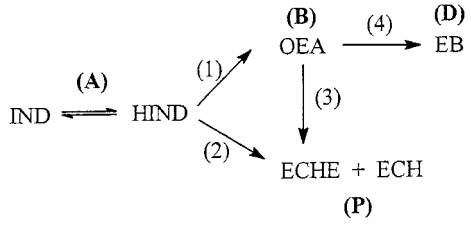

SCHEME 2. Simplified scheme for kinetic analysis.

TABLE 3

Reactivity of HIN vs IND and 2-MIN vs 2-MHIN

IND vs HIN				
			Conversion	
NiMo catalyst	Cpd	τ	TOT	HDN
	IND	0.444	0.257	0.173
	HIN	0.444	0.249	0.172
	IND	0.341	0.198	0.133
	HIN	0.341	0.206	0.140
	IND	0.222	0.122	0.078
	HIN	0.222	0.126	0.084
2-MIN vs 2-MHIN				
			Conversion	
CoMo catalyst	Cpd	τ	TOT	HDN
	2-MIN	0.634	0.129	0.121
	2-MHIN	0.634	0.126	0.118
	2-MIN	0.444	0.085	0.077
	2-MHIN	0.444	0.083	0.075
	2-MIN	0.277	0.050	0.041
	2-MHIN	0.277	0.063	0.055

perform a kinetic analysis on all reaction paths. However, initial rates of conversion of IND via the CNH path, $(r_{CNH})_0$, and the HYD path, $(r_{HYD})_0$, can be estimated to determine the effect of the methyl position on these two paths. Thus, according to Scheme 2, as $\tau \to 0$,

$$(r_{CNH})_0 = [dB/d\tau]_0, \quad [1]$$

$$(r_{HYD})_0 = [dP/d\tau]_0, \quad [2]$$

$$(r_{TOT})_0 = (r_{CNH})_0 + (r_{HYD})_0 = [dx/d\tau]_0, \quad [3]$$

where $(r_{TOT})_0$ is the total rate of indole disappearance, B is the mole fraction of OEA, P is the mole fraction of ECHE + ECH (the symbols also apply to the methylated products), x is the total conversion of IND or MIN, and τ is the space time. The rates in Eqs. [1]–[3] are in terms of feed flows, i.e., m^3/(kg min). Rates in terms of moles of IND or MIN are proportional to these and are obtained by multiplying by the constant feed concentration of 3.4×10^{-3} mol/m^3.

Plots of B, P, and x were extrapolated to $\tau = 0$ to obtain initial slopes, both by taking the tangent of the curve and by polynomial fitting. Although determining initial slopes from the limited data available is subject to some error, both methods were in reasonable agreement, with an estimated relative error of 15%. As an example, the mole fraction vs τ plots for IND are given in Fig. 3 for the CoMo catalyst. It is significant that the initial slope of the P vs τ plot is definitely not zero, confirming a direct route to P exists, i.e., the HYD pathway. If P were only generated from the CNH pathway (via OEA), the initial slope should approach zero. Similar results were obtained with the MINs.

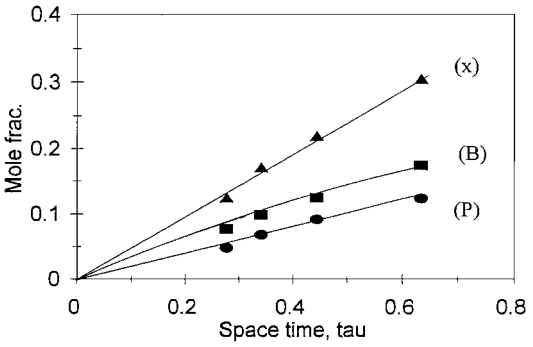

FIG. 3. Mole fractions vs space time for indole HDN. x, TOT conversion; B, OEA; C, ECHE + ECH (also methyl analogs).

The initial rates obtained for the various MINs are shown in Fig. 4 for the NiMo catalyst, where the values are in m^3/(kg min). The initial HYD rate $(r_{HYD})_0$ is faster than the CNH rate $(r_{CNH})_0$ for IND and methyl groups on the N ring, while the opposite occurs for Me groups on the aromatic ring. Compared to IND, the effect of the methyl position on the N ring is to lower the initial rates of both paths. However, for methyl groups on the aromatic ring, the CNH path is enhanced, whereas the HYD path is slightly decreased (5- and 7-positions), except for 6-MIN, which is not much different from IND.

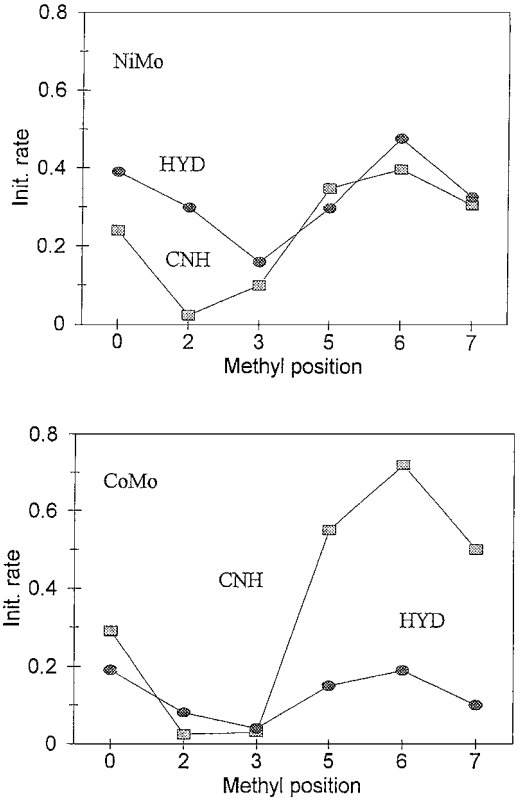

FIG. 4. Initial CNH and HYD rates vs methyl position.

The initial rates of the MINs for the CoMo catalyst are displayed in Fig. 4. Now, it is seen that the CNH rates are faster than the HYD rates. For methyl groups on the aromatic ring, the CNH rates are considerably enhanced, while the HYD rates are not, compared to IND. Again, both rates are decreased when a methyl group is on the N ring.

Catalyst activities cannot be compared directly because of different amounts of catalyst used. But initial rates can be compared since the catalyst weight is accounted for in the space time. In a comparison of the effect of methyl groups on the initial rates for the two catalysts, there are similarities in trends and differences in relative values. For both catalysts, generally the CNH rate is enhanced for methyls on the aromatic ring and depressed for methyls on the N ring. On the other hand, the order in the initial rates of the CNH and HYD paths for the two catalysts are reversed. Thus, the NiMo catalyst exhibits higher HYD vs CNH rates (except for 5-MIN), while the opposite pertains to the CoMo catalyst. Second, compared to CoMo, the NiMo catalyst exhibits higher HYD rates and lower CNH rates. This is in line with observations from many HDS studies (20), namely, that CoMo catalysts are superior for HDS (essentially a C–S bond breaking step) and NiMo for HDN (predominantly a HYD step). This also explains the relatively lower OEA yield for the NiMo catalyst. Considering the effect of the catalyst on the relative rates of the initial steps gives the following:

Path	Reaction	Init, rate
IND → OEA	CNH	NiMo < CoMo
IND → P	HYD	NiMo > CoMo
OEA → P	HYD	NiMo > CoMo

Consequently, the NiMo catalyst favors HYD over the CoMo catalyst, producing less OEA by all three paths. Although differences in catalyst formulations, e.g., loading, presence, or absence of phosphorous, may affect catalyst activities to some extent, it is believed that the remarkable differences in CNH and HYD rates between the NiMo and CoMo catalysts are predominantly due to the intrinsic nature of the promoter (Ni vs Co).

DISCUSSION

There is evidence in the literature that two separate pathways are involved in hydrotreating reactions of heterocyclic compounds, viz., one involving C–X (X is a heteroatom) bond cleavage and another hydrogenation (HYD) of the aromatic ring (13, 21–28). Many of these authors assumed that the two pathways require different sites. We propose that IND is adsorbed via the N atom on a CNH site and adsorption of IND occurs via the aromatic π system on a HYD site, although separate sites are not necessary to the following discussion. From theoretical calculations, Ruette *et al.* (29) showed that both σ- and π-adsorption modes are possible for pyridine adsorbed on a model MoS cluster. In the case of indole, direct adsorption through the N atom may not be favorable because the extra pair of electrons is shared in the π cloud of the N ring. A possible mode of adsorption could be through simultaneous adsorption of the N atom and the N ring on a dual site, leading to rapid hydrogenation of the C2–C3 double bond, freeing the electron pair for adsorption of the N atom on the CNH site.

According to Scheme 1, the first step in conversion of IND is its hydrogenation to HIN. As demonstrated above, conversion of IND to HIN is not rate-limiting for IND and 2-MIN, and presumably for the other MINs. Subsequently, HIN reacts via the two pathways, viz., the CNH path and the HYD path. For convenience, the following discussion is in terms of IND, but is intended to apply also to the MINs.

The CNH Pathway

Scheme 1 shows the steps involved in conversion of IND to OEA via this pathway. The second step, path 1, involves C–N bond cleavage and is assumed to be the rate-limiting step. The C–N cleavage reaction likely takes place by a Hofmann-type elimination mechanism (30). This involves proton transfer of an H^+ from a Bronsted site to the N atom, followed by C–N cleavage and β-elimination of an H atom to form an olefin (vinylaniline), which is rapidly hydrogenated to OEA. An alternate mechanism involving a nucleophilic substitution by catalyst SH^- (after formation of the charged N) leads to a similar result (12). Then, the enhancement in reactivity by a methyl group on the aromatic ring could be due to an inductive effect. Thus, the methyl group donates electrons to the aromatic ring, which in turn makes the N atom more negative, increases the proton transfer rate prior to C–N cleavage, and consequently increases the rate. For the methyl group on the N ring, once HIN is formed and the C2–C3 double bond becomes a single bond, methyls at the 2- or 3-position no longer exert an inductive effect. The methyl at the 2-position could possibly interfere with the transfer of the proton to the N atom. However, this fails to account for the low reactivity of 3-MIN.

For reaction via the CNH path, we propose adsorption via the N atom. Then, we may expect, in a general way, that reactivity should be related to the electrostatic potential (EP) on the N atom. Politzer and Murray (31) discuss the merits of using electrostatic potential for determining the interaction of a molecule with its environment. This correlation is based on the assumption that the CNH reaction proceeds when electrons on the N atom are coordinated to the active site. According to Perot (12), the C2 atom must be in sp^3 hybridization (HMIN) for C–N cleavage. Therefore, EP calculations were made for the HMIN structures. A plot of initial CNH rates vs EP(HMIN) is shown in Fig. 5 for the two catalysts. Rough trends are observed in both cases. The EPs do not vary much for all the HMINs, except for

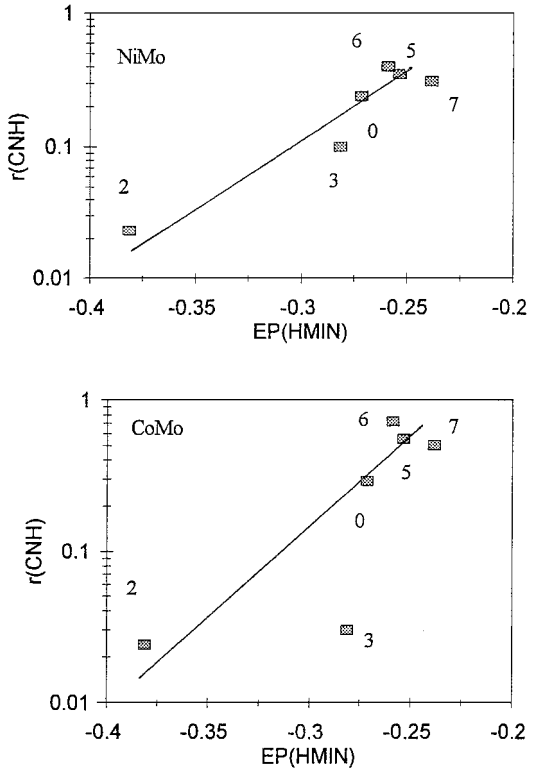

FIG. 5. Initial CNH rates vs EP for HMIN structures.

2-HMIN (which also exhibits the lowest CNH activity); thus, the effect of the methyl group on the N ring nearest to the N atom has the greatest effect on the EP. Although the correlation is reasonably good, the fit of the 3-MIN is appreciably off the line, especially for the CoMo catalyst. Actually, a better correlation was obtained using the EP values for the MINs instead of the HMINs, as seen in Fig. 6. This may be envisioned by supposing the adsorption mode proposed earlier involves a concerted reaction, with simultaneous hydrogenation of the C2–C3 double bond and adsorption through the N atom. Then, the controlling species would be the activated state of the MIN, rather than the HMIN.

In a study by Ma *et al.* (32), the desulfurization activity of a variety of sulfur compounds was related to the electron density of the HOMO on the sulfur atom, but the correlation was not applicable to the alkyldibenzothiophenes. Recently, Isoda *et al.* (33) reported a correlation between the desulfurization rate and the electron density of the HOMO-5 (molecular orbital five levels lower than the HOMO), which represents S–σ bonding. Both HOMO and HOMO-5, however, failed to give any correlation with the MIN rate data.

The HYD Pathway

Scheme 1 presents the steps involved in the conversion of IND to OHI and ultimately to ECHE. It is reasonable to suppose that the RLS is the hydrogenation of the aromatic ring (path 2), as the resonance energy of the aromatic system must be overcome.

The initial hydrogenation rate was somewhat lower for 5- and 7-MIN as compared to IND. It has been reported (34) that *o*- and *p*-alkyl-substituted phenols showed lower hydrogenation than phenol. It is noted that 7-MIN is *ortho* and 5-MIN is *para* to the N atom in indole, suggesting that a similar effect could be operative in the indole system. Furthermore, 6-MIN is more active for HYD than 5- and 7-MIN. Since the methyl group in 6-MIN is *meta* to the N atom, there appears to be a positive "*meta* effect", as also observed for the CNH path.

It has been reported (1) that the hydrogenation of the C_2–C_3 double bond of methyl-substituted benzothiophenes (MBT) is in the order BT > 2-MBT > 3-MBT, similar to our results with the analogous MINs (Fig. 1). Ma *et al.* reported (32) that the C_2–C_3 bond orders for the MBTs decrease in the above order, suggesting that the reactivity is directly related to the bond order of the C_2–C_3 bond. This implies that hydrogenation of IND to HIN is rate-controlling. However, this was not found to be the case in our calculations; bond orders of all MINs were found to be essentially the same, and our results (Table 3) showed this conversion was not rate-limiting under our conditions. Alternatively, once HMIN is formed by a rapid hydrogenation of the C_2–C_3 double bond, the N ring becomes puckered out of plane of the aromatic ring. Thus, part of the time, the approach of

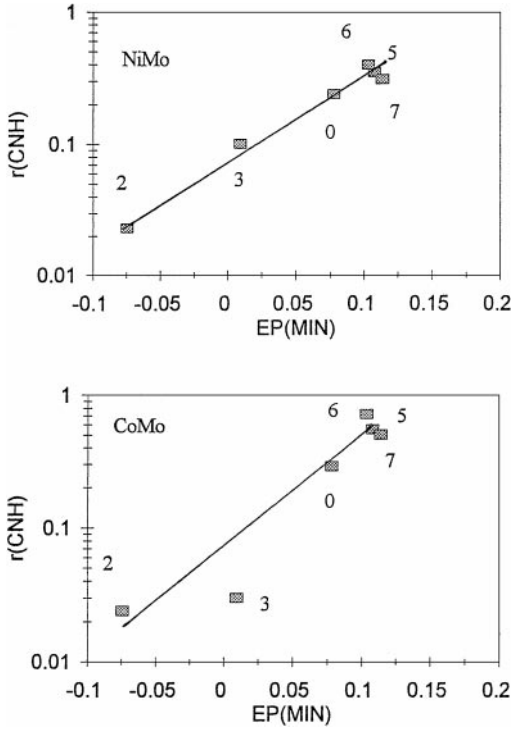

FIG. 6. Initial CNH rates vs EP for MIN structures.

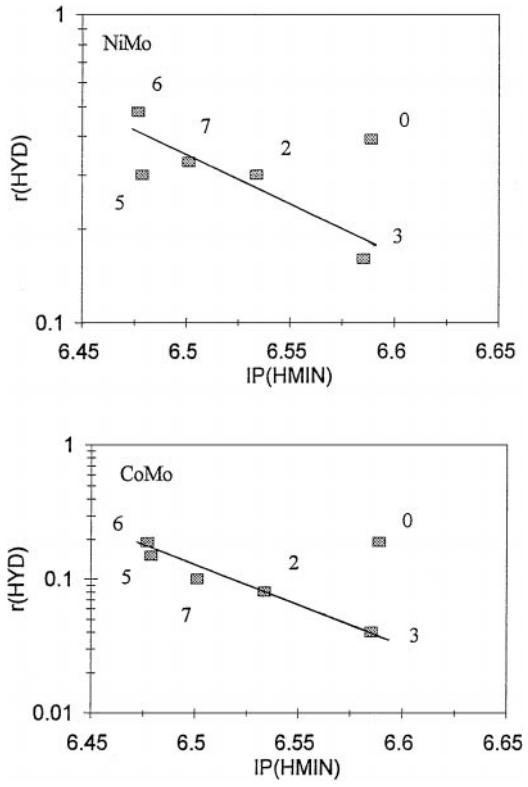

FIG. 7. Initial HYD rates vs IP for HMIN structures.

2- or 3-HMIN may be hindered from adsorption through the aromatic ring, and the overall rate of hydrogenation would be lowered. However, this fails to explain the lower HYD rate for 3-MIN compared to that for 2-MIN.

For reaction via the HYD path, we propose adsorption through the π system of the aromatic ring. Thus, we would expect that the reactivity should be related to the characteristics of the π complex. Nag (35) noted a correlation between hydrogenation activity of aromatic compounds and the ionization potential (IP). Plots of initial HYD rates of the MINs vs IP are given in Fig. 7 for the two catalysts. The correlation for the MINs is reasonable; the 2- and 3-MIN are in line. However, IND itself does not fit the correlation.

Final Comments

In the above attempts to rationalize methyl effects in terms of chemical properties of the MINs, the role of the catalyst, e.g., adsorption of the reactants and products, was ignored. Especially the differences in reactivities between NiMo and CoMo catalysts are not explicitly addressed in these correlations. Preliminary kinetic analysis of IND showed that IND is strongly adsorbed, while reaction products are relatively weakly adsorbed. Furthermore, analysis showed that different values for the adsorption constant of IND were obtained for the two pathways, indirect evidence for different sites. Therefore, different adsorption constants for the different MINs could have a bearing on their reactivity, inasmuch as this could lead to different concentrations of adsorbed MIN on the catalyst sites. Further investigation into the energetics of adsorption and reaction modes is clearly needed to shed more light on the role of the catalyst on these reactions.

CONCLUSIONS

1. The effect of a methyl group attached to the aromatic ring of indole is to increase the overall conversion compared to indole, while the opposite occurs for a methyl group on the N ring.
2. The initial conversion of indole and methyl indoles occurs by two parallel paths, a CNH path leading to an intermediate N compound and a HYD path leading to hydrogenated products.
3. The CNH path is enhanced by a methyl group on the aromatic ring, whereas the HYD path is relatively unaffected. Both paths are considerably lowered by methyl groups on the N ring.
4. The NiMo catalyst is superior to the CoMo catalyst for the HDN of indole by virtue of its relatively lower intermediate N-compound yield.
5. It may be difficult to achieve high HDN conversions for real feeds because of the very low reactivity of methyl groups on the N ring, a situation analogous to that of HDS of real feeds, where certain sulfur-containing compounds are resistant to HDS.

APPENDIX: NOMENCLATURE

B	intermediate N compound
CNH	carbon–nitrogen hydrogenolysis
EB	ethylbenzene
ECH	ethylcyclohexane
ECHE	ethylcyclohexene
EP	electrostatic potential
HDN	hydrodenitrogenation
HIN	indoline (dihydroindole)
HMIN	methyl-substituted dihydroindole
HYD	hydrogenation
IND	indole
IP	ionization potential
MIN	methyl-substituted indole
OEA	*o*-ethylaniline
P	hydrogenated products
TOT	total conversion of indole
τ	space time

ACKNOWLEDGMENTS

Support of this research by Haldor Topsøe A/S is gratefully acknowledged. We wish to thank Per Zeuthen for the GC/MS analyses. We also thank Dr. Patrick Redington for helpful discussions on computational chemistry methods.

REFERENCES

1. Ma, X., Sakanishi, K., and Mochida, I., *Ind. Eng. Chem. Res.* **35**, 2487 (1996).
2. Whitehurst, D. D., Isoda, T., and Mochida, I., *Adv. Catal.* **42**, 345 (1998).
3. Raje, A. P., Liaw, S. J., and Davis, B. H., *Appl. Catal. A* **150**, 319 (1997).
4. Geneste, P., Bonnet, M., and Graffin, P., *J. Catal.* **61**, 115 (1980).
5. Kwart, H., Schuit, G. C., and Gates, B. C., *J. Catal.* **61**, 128 (1980).
6. Kabe, T., and Ishihara, A., *Ind. Eng. Chem. Res.* **31**, 1577 (1992).
7. Isoda, T., Nagao, S., Karai, Y., and Mochida, I., *Am. Chem. Soc., Div. Pet. Chem.* **212**, 559 (1996).
8. Vanrysselberghe, V., and Froment, G. F., *Ind. Eng. Chem. Res.* **37**, 4231 (1998).
9. Cerny, M., *Colloid Czech. Chem. Commun.* **44**, 85 (1979).
10. Liaw, S.-J., Raje, A. P., Thomas, G. A., and Davis, B. H., *Appl. Catal. A* **150**, 343 (1997).
11. Bhinde, M. V., Ph.D. Dissertation, University of Delaware, 1979.
12. Perot, G., *Catal. Today* **10**, 447 (1991).
13. Olive, J.-L., Biyoko, S., Moulinas, C., and Geneste, P., *Appl. Catal.* **19**, 165 (1995).
14. Geneste, P., Moulinas, C., and Olive, J. L., *J. Catal.* **105**, 254 (1987).
15. Massoth, F. E., Balusami, K., and Shabtai, J., *J. Catal.* **122**, 256 (1990).
16. Callant, M., Holder, K. A., Grange, P., and Delmon, B., *Bull. Soc. Chim. Belg.* **104**, 245 (1995).
17. Zhang, L., and Ozkan, U. S., *Stud. Surf. Sci. Catal.* **101**, 1223 (1996).
18. Zhang, L., and Ozkan, U. S., *in* "Hydrotreatment and Hydrocracking of Oil Fractions" (G. F. Froment, B. Delmon, and P. Grange, Eds.), p. 69. Elsevier, New York, 1997.
19. Kim, S. C., Ph.D. Dissertation, University of Utah, Salt Lake City, Utah, 1999.
20. Topsøe, H., Clausen, B. S., and Massoth, F. E., "Catalysis-Science and Technology" (J. R. Anderson and M. Boudart, Eds.). Springer, New York, 1996.
21. Bhinde, M. V., Shih, S., Zawadski, R., Katzer, J. R., and Kwart, H., "Proceedings Third International Conference on the Chemistry and Uses of Molybdenum" (H. F. Barry and P. C. H. Mitchell, Eds.), p. 184. Climax Molybdenum Co., Ann Arbor, MI, 1979.
22. Satterfield, C. N., and Gultekin, S., *Ind. Eng. Chem. Process Des. Dev.* **20**, 62 (1981).
23. Odebunmi, E. O., and Ollis, D. F., *J. Catal.* **80**, 56 (1983).
24. Nagai, M., and Kabe, T., *J. Catal.* **81**, 440 (1983).
25. Gevert, B. S., Otterstedt, J.-E., and Massoth, F. E., *Appl. Catal.* **31**, 119 (1987).
26. Moreau, C., Aubert C., Durand, R., Zmimita, N., and Geneste P., *Catal. Today* **4**, 117 (1988).
27. van Gestel, J., Leglise, J., and Duchet, J.-C., *Appl. Catal. A* **92**, 143 (1992).
28. Vanryssel, V., and Froment, G. F., *Ind. Eng. Chem. Res.* **35**, 3311 (1996).
29. Ruette, F., Poveda, F. M., Sierraalta, A., Sanchez, M., and Rodriguez-Arias, E. N., *J. Mol. Catal.* **119**, 335 (1997).
30. Nelson, N., and Levy, R. B., *J. Catal.* **58**, 485 (1979).
31. Politzer, P., and Murray, J. S., *in* "Reviews in Computational Chemistry" (K. B. Lipkowitz and D. B. Boyd, Eds.) Vol. 2, Chap. 7. VCH Publishers, New York, 1991.
32. Ma, X., Sakamishi, K., Isoda, T., and Mochida, I., *Energy Fuels* **9**, 33 (1995).
33. Isoda, T., Takase, Y., Kusakabe, K., and Morooka, S., "Symposium on Chemistry of Diesel Fuels," 216th National Meeting, p. 575. American Chemical Society, Washington, DC, 1998.
34. Aubert, C., Durand, R., Geneste, P., and Moreau, C., *J. Catal.* **112**, 12 (1988).
35. Nag, N. K., *Appl. Catal.* **10**, 53 (1984).